Noise, channel and message identification on MIMO channels with general noise

Lucas Nogueira Ribeiro[4][0000-0002-9608-8750], João César Moura Mota[1][0000-0001-9890-2982],

Didier Le Ruyet[2] [0000-0002-9673-2075],

Eduardo Souza de Cursi[3] [0000-0001-9184-2489]

[1] GTEL, UFC, Campus du Pici, Fortaleza CE, Brazil
[2] CEDRIC, CNAM, 292 rue Saint Martin; 75141 Paris Cedex 03 - France
[3] LMN, Normandy University, INSA Rouen, 76801 St-Etienne du Rouvray CEDEX, France
[4]CRL, Ilmenau University of Technology, Ilmenau D-98684, Germany
souza@insa-rouen.fr

Abstract. This work presents an application of Uncertainty Quantification (UQ) approaches to a Multiple-Input Multiple-Output (MIMO) system. The use of UQ techniques in this field is new and is one of the originalities of the paper. A second originality of this work is to furnish an efficient method to deal with non-gaussian noise, with non-zero mean. A third originality is that the method proposed allows the estimation of the noise, of the channel and the decoding of messages - the approach makes all the chain: determination of the distribution of the noise, identification of the Channel Matrix and detection of the symbols transmitted. The first step is made by using UQ techniques, which furnish the distribution of the noise, without assumption of Gaussian distribution or a mean equal to zero. A new application of UQ techniques furnishes the channel matrix. Then, the detection of symbols is performed by a method based on the determination of a selection matrix formed by lines of the identity matrix. Numerical examples show that the proposed approach is practical and efficient.

Keywords: Uncertainty Quantification, Identification, MIMO systems.

1 Introduction

Multiple-input multiple-output (MIMO) systems involve a transmitter entity with multiple inputs which communicates with a receiver entity with multiple outputs. MIMO systems are typically adopted to describe many communication systems, including wireless [1], acoustic [2], and underwater systems [3-5]. These different communication scenarios are often deployed in uncontrolled and changing environments, hereafter referred to as communication channels. Therefore, the messages sent and received involve noise, measurement errors, and modeling errors that compromise proper decoding.

A widely adopted channel model in wireless communications is the Rayleigh fading [1, Chapter 3], wherein the received signals can be described in terms of a channel matrix

with Gaussian-distributed elements and an additive noise component. To ensure proper message detection, the receiver needs to correctly identify the channel matrix and the additive noise distribution by means of an adapted procedure. In many application scenarios, it is usually assumed that the noise has a Gaussian distribution and that its statistics are known a priori [6]. Scenarios with non-Gaussian additive noise [4, 5] are little explored in the literature, as well as scenarios where the noise is multiplicative so that the performance of MIMO symbol detectors is not fully understood in these scenarios yet.

In recent years, Uncertainty Quantification (UQ) proposed methods and tools to deal with general noise distributions, including non-Gaussian and multiplicative (see, for instance, [7-10]). These developments remain little exploited in the framework of Telecommunications. This work explores the use of UQ approaches to deal with noise in MIMO, namely for Channel and Noise Identification, then for Message decoding.

In the following, we present a novel pilot-based channel estimation method for a general additive noise, eventually non-Gaussian. As an example, we consider uniform and Laplace distributions, what shows that the approach is effective to calculate in non-Gaussian situations. These examples are chosen as an illustration, without loss of generality – other noise distributions can be assumed for the approach proposed. The UQ approach resumes as follows:

- In a first step, we determine the distribution of the noise, using a few measurements in "silent mode", where the transmitter does not transmit anything. UQ approach furnishes a fine estimation of the noise distribution from a small number of measurements, so that we obtain good estimates of the statistics of the noise from a few measurements.
- In a second step, we identify the channel matrix using a pilot method: the transmitter sends convenient pilot symbols that allows the receiver to identify successively each column of the matrix channel individually.
- Finally, we use the results of these steps to decode messages and we analyze the error rate in some situations, with different alphabets.

2 System Model

Let us consider a single-user multiple-input multiple-output (MIMO) system with N_t transmission and N_r reception antennas. Under the flat fading assumption, the discrete-time received signal vector $\boldsymbol{y} \in \mathbb{C}^{N_r}$ is given by

$$\boldsymbol{y} = \boldsymbol{H}\boldsymbol{x} + \boldsymbol{n}, \tag{1}$$

where $\boldsymbol{x} \in \mathbb{C}^{N_t}$ is the vector of the transmitted signal, $\boldsymbol{H} \in \mathbb{C}^{N_r \times N_t}$ is the channel matrix, and $\boldsymbol{n} \in \mathbb{C}^{N_r \times 1}$ is a vector of additive noise. Assuming independent and identically distributed (i.i.d.) Rayleigh fading, the elements of $\boldsymbol{H}$ are i.i.d. complex Gaussian random variables with zero mean and unit variance. Each transmitted signal $\boldsymbol{x_n}$, $n = 1, \ldots, N_t$, consists of a digitally-modulated symbol in the constellation alphabet $\boldsymbol{a}$, of order M: $\boldsymbol{a} = (a_1, \ldots, a_M) \in \mathbb{C}^M$.

If convenient, the complex-valued signal model (1) may be rewritten in terms of its real and imaginary parts as follows:

$$\overline{\boldsymbol{y}} = \overline{\boldsymbol{H}}\overline{\boldsymbol{x}} + \overline{\boldsymbol{n}} \tag{2}$$

with

$$\overline{\boldsymbol{y}} = \begin{pmatrix} \boldsymbol{y_{re}} \\ \boldsymbol{y_{im}} \end{pmatrix},\ \overline{\boldsymbol{H}} = \begin{pmatrix} \boldsymbol{H_{re}} & \boldsymbol{-H_{im}} \\ \boldsymbol{H_{im}} & \boldsymbol{H_{re}} \end{pmatrix},\ \overline{\boldsymbol{x}} = \begin{pmatrix} \boldsymbol{x_{re}} \\ \boldsymbol{x_{im}} \end{pmatrix},\ \overline{\boldsymbol{n}} = \begin{pmatrix} \boldsymbol{n_{re}} \\ \boldsymbol{n_{im}} \end{pmatrix} \tag{3}$$

Here, we denote $\boldsymbol{\xi_{re}} = Re(\boldsymbol{\xi})$ and $\boldsymbol{\xi_{im}} = Im(\boldsymbol{\xi})$. Thus, $\overline{\boldsymbol{y}} \in \mathbb{R}^{2N_r}$, $\overline{\boldsymbol{H}} \in \mathbb{R}^{2N_r \times 2N_t}$, $\overline{\boldsymbol{x}} \in \mathbb{R}^{2N_t}$, $\overline{\boldsymbol{n}} \in \mathbb{R}^{2N_r}$, which are real-valued vectors corresponding to the received signal, the channel matrix, the transmitted signal, the additive noise, respectively.

3 Determination of the distribution of the noise

As previously observed, the determination of the distribution of the noise may be performed in a "silent mode", where the transmitter does not transmit anything. In this case, the signal $\boldsymbol{x}$ in Eq. (1) becomes $\boldsymbol{x} = \boldsymbol{0}$, so that $\overline{\boldsymbol{x}} = \boldsymbol{0}$ in Eq. (2). The received message is $\boldsymbol{y} = \boldsymbol{n}$, $\overline{\boldsymbol{y}} = \overline{\boldsymbol{n}}$. Taking s measurements, we generate a sample $\mathcal{N} = \{\boldsymbol{n^1}, \dots, \boldsymbol{n^s}\}$ of the noise, which is brought to a matrix $\boldsymbol{N} = (\boldsymbol{n^1}, \dots, \boldsymbol{n^s}) \in \mathbb{C}^{N_r \times s}$ having as columns the measurements for each realization: $N_{ij} = \boldsymbol{n_j^i}$. The noise measurements are also expanded into real and imaginary parts:

$$\overline{\boldsymbol{N}} = \begin{pmatrix} \boldsymbol{Re}(\boldsymbol{n^1}) & \cdots & \boldsymbol{Re}(\boldsymbol{n^s}) \\ \boldsymbol{Im}(\boldsymbol{n^1}) & \cdots & \boldsymbol{Im}(\boldsymbol{n^s}) \end{pmatrix} \in \mathbb{R}^{2N_r \times s} \tag{4}$$

Using the UQ approach, we consider a Hilbert basis $\Phi = \{\varphi_n : n \in \mathbb{N}\}$ and a random variable U (for instance, uniform or Gaussian). Assuming that the noise has a finite second moment (i. e., that the noise is square summable), we have

$$\overline{N}_i \approx \sum_{j=0}^{+\infty} c_{ij}\varphi_j(U) \tag{5}$$

In practice, we approximate the noise using a finite sum, truncated at order k:

$$\overline{N}_i \approx \sum_{j=0}^{\mathrm{k}} c_{ij}\varphi_j(U) \tag{6}$$

Let us introduce

$$\boldsymbol{C} = \left(c_{ij} : 1 \le i \le N_r, 1 \le j \le k\right),\ \boldsymbol{\Phi}(\mathrm{U}) = \begin{pmatrix} \varphi_0(\mathrm{U}) \\ \vdots \\ \varphi_k(\mathrm{U}) \end{pmatrix}.$$

Then

$$\bar{N}_i = \left(\boldsymbol{C}\boldsymbol{\Phi}(U)\right)_i \tag{7}$$

Notice that, a priori, the random variable U is different for each index i. The coefficients $\boldsymbol{C}$ must be determined by one of the following UQ methods: collocation, variational approximation, moments matching. (See [10] for a detailed description). As an example, let us assume that $\bar{N}_1$ is uniformly distributed on $(-1, 1)$ and we have $s = 20$ measurements of $\bar{N}_1$: $\{\bar{N}_1^1, \dots, \bar{N}_1^{20}\}$:

Table 1. Measurements of $\bar{N}_1$

-0.0924	-0.0827	-0.0715	-0.0621	-0.0566	-0.0529	
-0.0158	-0.0133	0.0032	0.0083	0.0151	0.0193	0.0285
0.0291	0.0297	0.0581	0.0807	0.0812	0.0828	0.0938

Let U_1 be Gaussian $N(0,1)$. We consider a sample from U_1 :

Table 2. A sample of 20 variates from the Gaussian distribution (randomly generated)

-1.5932	-1.0216	-0.7483	-0.6147	-0.2585	0.2510	
0.0180	0.1335	0.1954	0.2398	0.3041	0.5680	0.6214
0.6324	0.7506	0.8446	1.1717	1.2247	1.2325	1.5017

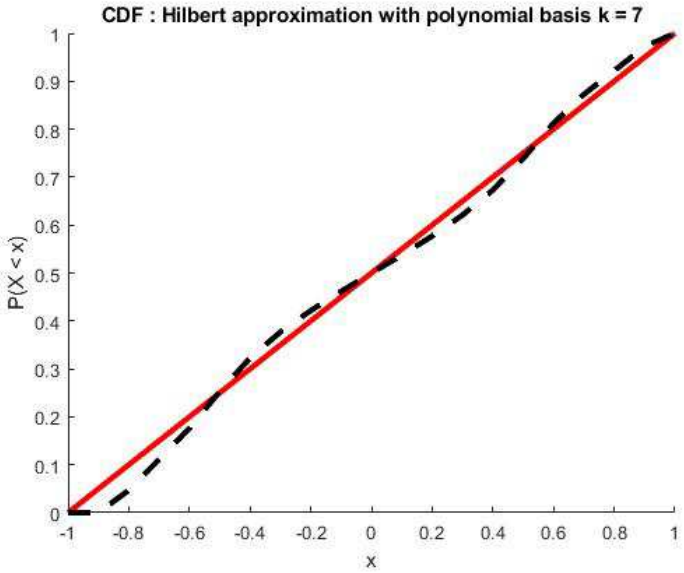

Fig. 1. Hilbert approximation of a noise. The noise is uniformly distributed, but we consider a Gaussian variable in the expansions (5)-(6). The results are obtained by Moments Matching for the first 8 moments ([4]).

We apply the UQ approach with a polynomial basis

$$\varphi_j(U) = \left(\frac{U-a}{b-a}\right)^{\mathrm{i}-1} \tag{8}$$

where $a = \min(U)$ and $b = \max(U)$. We take $k = 9$ (thus, the degree of the polynomial is 9). By using the Moments Matching Approach [4], with 8 moments, we obtain the coefficients given in **Table 3**:

Table 3. Coefficients of the polynomial

$i = 0$	$i = 1$	$i = 2$	$i = 3$	$i = 4$
-0.0927	9.416	-181.460	1449.778	-6246.36
$i = 5$	$i = 6$	$i = 7$	$i = 8$	$i = 9$
15937.485	-24760.923	22981.886	-11704.300	2514.663

As soon as the coefficients are obtained, we use the polynomial to generate a large sample formed by 1e4 variates from $\bar{N}_1$. This large sample is used to generate an empirical CDF of $\bar{N}_1$. The resulting CDF is shown in **Figure 1** above. Notice that, despite the use of a Normal Variable in the expansion (5)-(6), the resulting distribution is close to a Uniform Variable.

As an example, let us consider a 8×8 −MIMO System ($N_r = N_t = 8$) such that the noise is additive and distributed as follows:

- in the real part, it is uniformly distributed with mean -0.03 and variance 0.1;
- in the imaginary part follows a Laplace's distribution having a mean 0.02 and a variance 0.1;
- The components of the noise are mutually independent.

These assumptions do not imply a loss of generality: indeed, the approach applies to arbitrary noises of finite variance, including dependent components. It is also possible to introduce a given covariance matrix as constraint to be verified.

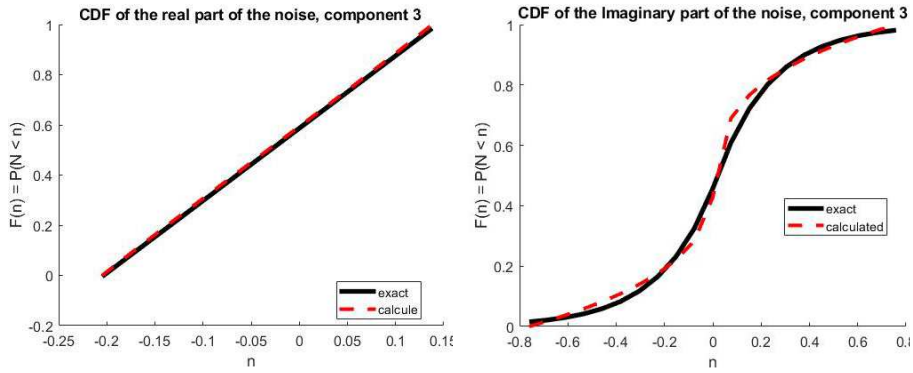

Fig. 2. Determination of the distribution of the noise: a typical result. Results for component 3: at left, the CDF of the real part; at right the CDF of the imaginary part

Let us consider 250 measurements of the noise. We use the approach by collocation ([4]) with a polynomial basis involving $k = 3$ (thus, a polynomial of degree 3) and U uniformly distributed on (0,1). By this way, we determine the coefficients $(c_{in} : 1 \leq i \leq 16, 0 \leq n \leq 3)$ of the approximation, which is, then, used to generate a large sample of $1e4$ variates from each component of the noise. The large sample is used to generate the empirical distribution of the noise. The results obtained correspond to an error of 3.5 % in the CDF of the noise. We show above (**Figure 2**) a typical result – which are analogous for the other components.

The results may be improved by using, on the one hand, a larger number of measurements and, on the other hand, by using the approach by moment matching. For instance, for 1000 measurements, the error in the CDF is of 1.6 %. The mean of the real part of the noise is estimated by the empirical mean of the large sample. We obtain the results shown in **Table 4**. As we may observe, the results are close to the real means.

Table 4. Empirical means for each component (in ascending order: at left, the first component; at right, the 8th. one)

Real	-0.032	-0.030	-0.028	-0.027	-0.023	-0.032	-0.030	-0.023
Imaginary	0.034	0.027	0.019	0.021	0.033	0.043	0.029	0.012

To get some statistics about the behavior of the proposed method, we realized 1000 approximations using different realizations of the noise and we analyzed the distributions of the errors. We determined the empirical CDF by the same way as the one upper described: a Hilbert approximation by a polynomial of degree 4, then the generation of a sample of $1e4$ variates. The sample is used to determine the CDF. The PDF is found by particle derivation of the CDF (see [11]).

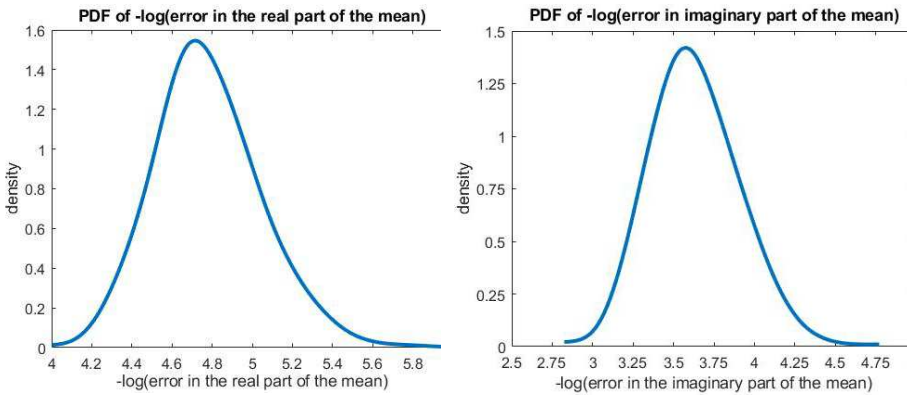

Fig. 3. PDF of $-\log(error)$ for the real (at left) and the imaginary (at right) parts of the mean (natural logarithm)

In **Figure 3** above, we exhibit the PDF obtained for the negative natural logarithms of the errors in the real and the imaginary parts of the mean of the noise (recall that it is not equal to zero): notice that the larger is the abscissa, the smaller is the error. We observe that both the distributions are unimodal. The mode for the real part is about 4.8 and the mode for the imaginary part is about 3.6. Indeed, the statistics of the errors in the original sample of 1000 realizations are given in the **Table 5** below

Table 5. Statistics of the errors in the estimation of the mean of the noise. These values correspond to about 3.6 % of error in the real part and 11 % in the imaginary part.

	Mean	Standard Deviation
Real part	0.0087	0.0021
Imaginary part	0.0273	0.0070

We observe that the errors are larger in the imaginary part: this is connected to the original probability distribution: indeed, the estimation of the Laplace distribution mean appears to be harder. Improvements may be obtained by using other approaches, such as other Hilbert basis leading to approximations that are more accurate.

4 Channel Estimation

The standard procedure for the estimation of the channel matrix involves the exchange of *pilot signals*– i. e., reference signals known both by the transmitter and receiver: the transmitter sends a N_p-length sequence of reference signals $\boldsymbol{p^1}, \dots, \boldsymbol{p^{N_p}}$ (the *pilots*). Then, the comparison with the received signals $\boldsymbol{y^i} = \boldsymbol{Hp^i} + \boldsymbol{n^i}, i = 1, \dots, N_p$ furnishes information about the channel matrix $\boldsymbol{H}$.

One of the limitations of this procedure is the necessary knowledge of the distribution of the noise $\boldsymbol{n}$: indeed, let $\boldsymbol{P} = \left(\boldsymbol{p^1}, \dots, \boldsymbol{p^{N_p}}\right) \in \mathbb{C}^{N_t \times N_p}$ denote the *pilot matrix*, having the pilots as columns. Then, the signals received may be collected in a matrix $\boldsymbol{Y} = (y^1, \dots, y^{N_p}) \in \mathbb{C}^{N_r \times N_p}$ given by

$$\boldsymbol{Y} = \boldsymbol{HP} + \boldsymbol{N} \tag{9}$$

where $\boldsymbol{N} = \left(\boldsymbol{n^1}, \dots, \boldsymbol{n^{N_p}}\right) \in \mathbb{C}^{\boldsymbol{N_r} \times \boldsymbol{N_p}}$ is the additive noise matrix, having as columns the noise corresponding to each pilot. The least squares (LS) channel estimation based on Eq. (4) is given by

$$\widehat{\boldsymbol{H}}_{LS} = \boldsymbol{Y}\boldsymbol{P}^{\dagger} \tag{10}$$

where $\boldsymbol{P}^{\dagger}$ is the generalized inverse of $\boldsymbol{P}$. We have $\boldsymbol{P}^{\dagger} = \boldsymbol{P}^{*}(\boldsymbol{P}\boldsymbol{P}^{*})^{-\boldsymbol{1}} \in \mathbb{C}^{\boldsymbol{N_p} \times \boldsymbol{N_t}}$, where $\boldsymbol{P}^{*} \in \mathbb{C}^{\boldsymbol{N_p} \times \boldsymbol{N_t}}$ is the Hermitian adjoint matrix associated to $\boldsymbol{P}$. Notice that the existence of $\boldsymbol{P}^{\dagger}$ assumes that $\boldsymbol{P}\boldsymbol{P}^{*} \in \mathbb{C}^{\boldsymbol{N_t} \times \boldsymbol{N_t}}$ is invertible – thus, $\boldsymbol{P}$ has full row rank N_t and $(N_p \geq N_t)$.

$$\widehat{\boldsymbol{H}}_{LS} = \boldsymbol{H} + \boldsymbol{P}^{\dagger}\boldsymbol{N}\,, \tag{11}$$

8

so that the result contains noise. To eliminate – or simply reduce – the effect of the noise, some information about its distribution is required. For instance, a minimum mean square error (MMSE) estimator can be devised if convenient statistics of the signals and noise are available.
In many application scenarios, it is reasonable to assume that the additive noise has a complex-valued Gaussian distribution. Moreover, it is usual to assume that the noise statistics are known a priori. Scenarios where the additive noise is not Gaussian-distributed are little explored in the literature and the performance of MIMO symbol detectors is not fully understood yet.

In the recent years, UQ proposed methods and tools to deal with general distributions of probability: for instance – as previously remarked - the approach presented in section 3 deals with any distribution having a finite variance. The UQ approach may be employed to improve the identification of the Channel Matrix by two basic procedures, described and illustrated in the sequel.
In the first one, the distribution of $\boldsymbol{n}$ is determined as shown in section 3. Then, the information obtained is used to improve the estimation given in Eq. (9): denoting by $E(\blacksquare)$ the mean, we have

$$E\left(\widehat{\boldsymbol{H}}_{LS}\right) = \boldsymbol{H} + \boldsymbol{P}^{\dagger}\boldsymbol{E}(\boldsymbol{N}) \tag{12}$$

Thus, we may generate a sample $\boldsymbol{Y^1}, \ldots \boldsymbol{Y^{N_s}}$ from $\boldsymbol{Y}$ to estimate

$$E\left(\widehat{\boldsymbol{H}}_{LS}\right) = E(\boldsymbol{Y})\boldsymbol{P}^{\dagger} \approx \left(\frac{1}{\mathrm{N_s}}\sum_{j=1}^{\mathrm{N_s}} \mathbf{Y^j}\right)\boldsymbol{P}^{\dagger} \tag{13}$$

and

$$E(N_i) \approx \frac{1}{N_u}\sum_{\boldsymbol{r=1}}^{\boldsymbol{N_u}}\left(\boldsymbol{C\Phi}(U_r)\right)_i = \frac{1}{N_u}\sum_{r=1}^{\boldsymbol{N_u}}\sum_{j=0}^{\mathrm{k}} c_{ij}\varphi_j(U_r) \tag{14}$$

may be estimated using a large sample of N_U variates from U. Then, we obtain $\boldsymbol{H}$ from Eq. (12).

The second approach consists in applying the UQ procedures directly to $\boldsymbol{Y}$: we may consider the expansion

$$\mathrm{Y}_i = \sum_{j=0}^{+\infty} y_{ij}\varphi_j(U) \approx \sum_{j=0}^{\mathrm{k}} y_{ij}\varphi_j(U) \tag{15}$$

Then, we may estimate

$$E\left(\widehat{\boldsymbol{H}}_{LS}\right) = \boldsymbol{E}(\boldsymbol{Y})\boldsymbol{P}^{\dagger} \tag{16}$$

and get $\boldsymbol{H}$ from Eq. (12).

As an example, let us consider the situation where the Channel Matrix has real and imaginary parts given in **Tables 6 and 7**

Table 6. Real part $\boldsymbol{H_{re}}$ of the test channel matrix

0.3802	2.5303	-0.0878	0.3457	-0.7558	-0.0723	0.7731	-0.5442
1.2968	1.9583	1.0534	0.7316	-0.5724	-0.1707	0.7844	0.2626
-1.5972	-0.9545	0.9963	0.5140	-2.0819	0.2257	-0.6107	-0.1595
0.6096	2.1460	1.0021	-0.2146	1.0171	0.2212	0.0547	0.7901
0.2254	0.5129	0.4748	0.2078	0.2299	-0.6116	-0.8585	-0.7701
-0.9247	-0.0446	-0.8538	-0.5567	-0.5338	-0.0212	-0.7874	0.0230
-0.3066	0.5054	0.5072	0.6282	0.9689	-0.1166	-0.0048	0.3907
0.2423	-0.1449	1.1528	-0.8111	-1.2102	0.4439	1.0837	0.7782

Table 7. Imaginary part $\boldsymbol{H_{im}}$ of the test channel matrix

1.0919	-0.1361	1.0036	0.1525	-0.0583	0.2146	0.9578	2.0563
0.0608	0.6283	0.2062	-0.8244	-1.3669	-0.4245	-0.7581	0.5835
-1.0547	-0.5408	0.1399	-0.8117	-0.3104	0.3465	0.6795	0.9751
-0.5249	-0.9916	1.1227	0.0742	-1.2690	0.5228	0.0877	-0.7482
-0.7507	-1.0058	-0.5688	0.5107	0.5942	1.2105	1.0159	-0.3314
1.6620	0.3452	0.4926	1.8282	-0.6279	-0.1373	-1.3866	-0.1927
-0.4353	-0.1254	-0.5905	-0.4716	0.0708	-1.5120	-0.1398	0.7767
0.5290	-0.1386	-0.1723	0.1325	-0.3850	-0.5937	-0.8541	-0.1965

To simplify the procedure, we consider the successive identification of the columns of $\boldsymbol{H}$ – there is no loss of generality, since the UQ procedures apply to the complete matrix $\boldsymbol{H}$. To perform the identification of the first column, we consider as pilot

$$\boldsymbol{P} = \left(\boldsymbol{p^1}, \dots, \boldsymbol{p^{N_p}}\right), \qquad \boldsymbol{p^i} = \begin{pmatrix} 1 \\ 0 \\ \dots \\ 0 \end{pmatrix}$$

Let us denote $\boldsymbol{H^1}$ the first column of $\boldsymbol{H}$. Then,

$$\boldsymbol{Y} = \boldsymbol{HP} + \boldsymbol{N} = \left(\boldsymbol{H^1} + \boldsymbol{n^1} \quad \dots \quad \boldsymbol{H^1} + \boldsymbol{n^{N_p}}\right),$$

so that we obtain a noisy sample of N_p variates from $\boldsymbol{Y^1} = \boldsymbol{H^1} + \boldsymbol{n}$. Let us apply the first procedure defined above: we have

$$\boldsymbol{H^1} \approx \frac{1}{N_p} \sum_{\boldsymbol{r=1}}^{\boldsymbol{N_p}} \boldsymbol{Y^r} - \boldsymbol{E(N)},$$

where $\boldsymbol{E(N)}$ is estimated by using Eq. (14). The procedure may be iterated for all the columns of the matrix $\boldsymbol{H}$, leading to the complete determination of the Channel matrix.

The total number of messages requested for the identification is $N_t \times N_p$ (N_p messages for each column)

Let us consider again the same 8×8 −MIMO System introduced in section 3, with additive noise uniformly distributed in the real part of $\boldsymbol{H}$ and Laplace distributed in the imaginary part of $\boldsymbol{H}$. We use 1000 measurements to determine the distribution of the noise and $N_p = 100$. To obtain some statistics about the behavior of the proposed method, we realized 1000 identifications using different realizations of the noise and we analyzed the distributions of the errors. In general, the first procedure furnishes a result with errors of about 2.5 %. Typical results are shown in **Tables 8 and 9**.

Table 8. A typical result for the identification of $\boldsymbol{H_{re}}$: the relative error is 2.5 %. In this case, we used a polynomial of degree 3 ($k = 3$)

0.3197	2.5331	-0.1123	0.3573	-0.7387	-0.0688	0.7639	-0.5622
1.3180	1.9880	1.0252	0.7476	-0.5982	-0.1660	0.8447	0.2547
-1.5747	-0.9262	0.9858	0.5271	-2.0471	0.2200	-0.6355	-0.1403
0.6090	2.1529	1.0666	-0.2134	1.0019	0.2164	0.0477	0.7759
0.2145	0.4843	0.4695	0.2636	0.2107	-0.6655	-0.8945	-0.7468
-0.9401	-0.0512	-0.8667	-0.5595	-0.5474	-0.0765	-0.7875	0.0107
-0.2738	0.5069	0.5372	0.6183	0.9725	-0.1592	-0.0099	0.3689
0.2243	-0.1180	1.1575	-0.8363	-1.2034	0.4597	1.1054	0.7495

Table 9. A typical result for the identification of $\boldsymbol{H_{im}}$: the relative error is 2.7 %. In this case, we used a polynomial of degree 5 ($k = 5$)

1.1223	-0.1371	1.0276	0.1651	-0.0996	0.2413	0.9847	2.0552
0.0900	0.5813	0.2079	-0.8344	-1.4037	-0.3948	-0.8001	0.5528
-1.0403	-0.5373	0.1504	-0.7784	-0.3145	0.3370	0.6600	1.0037
-0.5472	-1.0040	1.1498	0.0735	-1.3057	0.4959	0.0892	-0.7480
-0.7535	-1.0056	-0.6029	0.5181	0.5898	1.1942	1.0119	-0.2977
1.6606	0.3181	0.4542	1.7691	-0.6316	-0.1724	-1.3636	-0.2176
-0.4341	-0.1186	0.5958	-0.4734	0.1117	-1.5063	-0.1536	0.7360
0.5280	-0.1820	-0.1652	0.1276	-0.3488	-0.5760	-0.8474	-0.1550

Analogously to the noise, we generated statistics about the behavior of the proposed method: 1000 approximations using different realizations of the noise were used to determine the empirical CDF by the same way as preceding: a Hilbert approximation by a polynomial of degree 4, then the generation of a sample of $1e4$ variates. As in the study of the noise, the sample is used to determine the CDF and the PDF is found by particle derivation of the CDF ([11]).

In **Figure 4** below, we exhibit the PDF obtained for the relative errors in the real and the imaginary parts of the channel matrix. Again, both the distributions are unimodal. The mode for the real part is about 2.5 % and the mode for the imaginary part is about

3.5 %. Indeed, the statistics of the errors in the original sample of 1000 realizations are given in the **Table 10** below

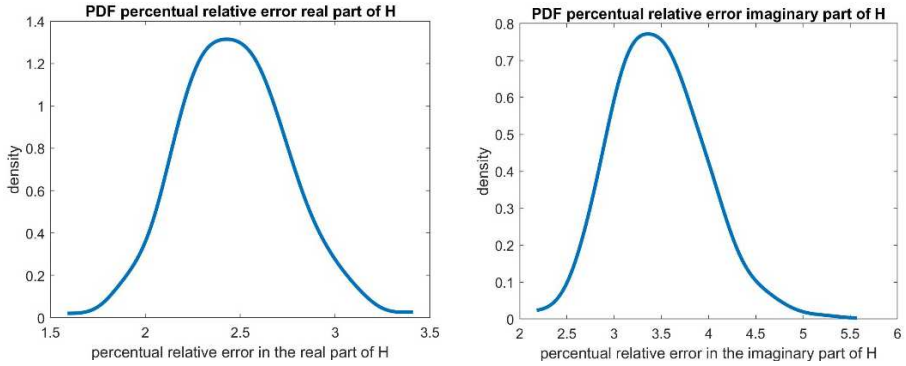

Fig. 4. PDF of the relative errors for the real and the imaginary parts of $\boldsymbol{H}$ (first approach)

Table 10. Statistics of the relative errors in the estimation of the channel matrix. These values correspond to about 2.5 % of error in the real part and 3.5 % in the imaginary part (first approach)

Quantity	Mean	Standard Deviation
Percent error in $\boldsymbol{H}_{re}$	2.4666	0.2804
Percent error in $\boldsymbol{H}_{im}$	3.4772	0.4861

Again, the errors are larger in the imaginary part, due to the difficulty introduced by the Laplace distribution. Here yet, improvements may be obtained by using other approaches, such as other Hilbert basis leading to more accurate approximations.

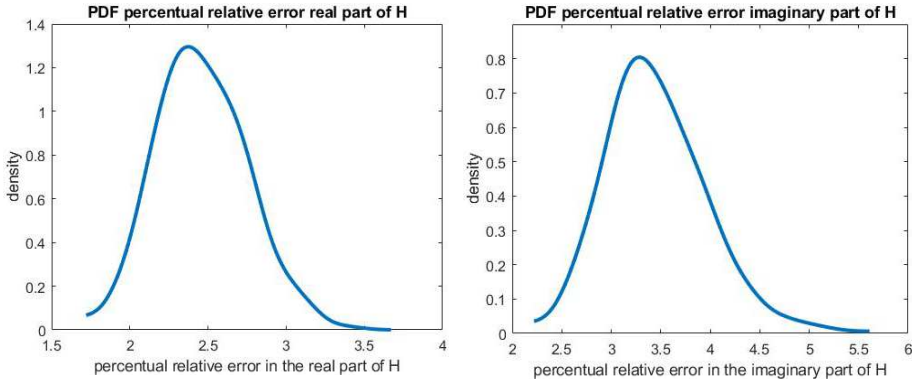

Fig. 5. PDF of the relative errors for the real and the imaginary parts of $\boldsymbol{H}$ (second approach)

Now, let us consider the second approach: as previously mentioned, the UQ procedures are applied directly to $\boldsymbol{Y}$. The results are given in **Tables 11,12, 13** below. We observe that the results are close to the preceding ones.

Table 11. Statistics of the errors in the estimation of the channel matrix. These values correspond to about 2.5 % of error in the real part and 3.5 % in the imaginary part (second approach)

Quantity	Mean	Standard Deviation
Percent error in $\boldsymbol{H}_{re}$	2.4632	0.2861
Percent error in $\boldsymbol{H}_{im}$	3.4593	0.5047

Table 12. A typical result for the identification of $\boldsymbol{H}_{\boldsymbol{re}}$: the relative error is 2.7 %. In this case, we used a polynomial of degree 3 ($k = 3$)

0.3680	2.5028	-0.0990	0.3692	-0.7568	-0.1403	0.7332	-0.4937
1.2847	1.9414	1.0555	0.7532	-0.6005	-0.2234	0.7769	0.2865
-1.5988	-0.9406	0.9933	0.5163	-2.0528	0.2602	-0.6184	-0.1595
0.5886	2.1526	1.0214	-0.2446	1.0243	0.2035	0.0250	0.7791
0.2338	0.4664	0.4736	0.1865	0.2833	-0.6027	-0.8558	-0.7494
-0.9310	-0.0365	-0.8368	-0.5052	-0.5354	0.0047	-0.7993	0.0442
-0.2799	0.5414	0.5156	0.6768	0.9260	-0.1125	0.0092	0.3585
0.2214	-0.1848	1.1550	-0.8090	-1.2271	0.4246	1.0873	0.7406

Table 13. A typical result for the identification of $\boldsymbol{H}_{\boldsymbol{im}}$: the relative error is 3.04 %. In this case, we used a polynomial of degree 5 ($k = 5$)

1.0586	-0.1284	1.0096	0.1549	-0.0503	0.2289	0.9755	2.0566
0.0730	0.6450	0.2133	-0.8185	-1.3692	-0.4237	-0.7618	0.6284
-1.0485	-0.5586	0.1311	-0.8217	-0.2576	0.3661	0.6772	1.0161
-0.5068	-0.9969	1.1592	0.0935	-1.2508	0.5323	0.0611	-0.7377
-0.7666	-1.0275	-0.5537	0.5166	0.5941	1.2245	0.9634	-0.3507
1.6436	0.3618	0.4758	1.8125	-0.5872	-0.1457	-1.4069	-0.1555
-0.4201	-0.1268	0.6263	-0.5105	0.0407	-1.5517	-0.1747	0.7578
0.4866	-0.1457	-0.1615	0.0918	-0.3937	-0.6077	-0.8930	-0.2004

5 Symbol Detection

At this stage, we obtained information about the distribution of the noise and about the channel matrix. The next step is the detection of symbols. Let us assume that both the real and imaginary parts of the symbols are chosen in an alphabet $\boldsymbol{a}$ corresponding to the so-called Quadrature Amplitude Modulation (QAM) of order $M = 2^d$: $\boldsymbol{a} = (a_1, \dots, a_M) \in \mathbb{C}^M$, with

$$a_i = -2^d + 2i - 1 : 1 \leq i \leq 2^d .$$

For $d = 1$, we have $\boldsymbol{a} = (-1, 1)$. For $d = 2$, $\boldsymbol{a} = (-3, -1, 1, 3)$. In the general situation:

$$\boldsymbol{a} = (-2^d + 1, -2^d + 3, \dots, -1, 1, 3, \dots, 2^d - 3, , 2^d - 1\ ) .$$

Let us consider the situation where each transmitter sends a symbol: for the 8×8 −MIMO System introduced in section 3, the transmitters send 8 symbols and the receivers receive 8 values, modified by the channel matrix and the noise. The aim is to determine the symbols sent by the transmitters using the values detected by the receivers, the estimation of the channel matrix and our knowledge about the distribution of the noise.

In the sequel, we consider two methods of detection. The first approach associates each symbol to a vector of length M, corresponding to lines of the $M \times M$ identity matrix:

$$\boldsymbol{a_i} = (s_{i1}, \dots, s_{iM}),\ s_{ij} \in \{0,1\},\ s_{ii} = 1, s_{ij} = 0\ if\ i \neq j\ .$$

Thus, an unknown symbol a corresponds to an unknown line of the $M \times M$ identity matrix, i. e., to a vector

$$\boldsymbol{a} = (z_1, \dots, z_M), \qquad z_i \in \{0,1\},\ z_1 + \cdots + z_M = 1\ .$$

According to these observations, N_t unknown real symbols are equivalent to N_t unknown lines of the $M \times M$ identity matrix, i.e., to N_t unknown vectors of length M. Thus, we have $N_t \times M$ unknowns to be determined. These unknowns are collected into a $N_t \times M$ matrix $\boldsymbol{Z} = \left(z_{ij}: 1 \leq i \leq N_t, 1 \leq j \leq M\right)$, having as lines the vectors corresponding to the unknown symbols. Analogously to Eqs. (2) – (3), we may consider separately the real and imaginary parts of the symbols, so that the message transmitted, and the data received read as

$$\bar{\boldsymbol{x}} = \bar{\boldsymbol{Z}}\bar{\boldsymbol{a}}\ ;\ ;\quad \bar{\boldsymbol{y}} = \bar{\boldsymbol{H}}\bar{\boldsymbol{Z}}\bar{\boldsymbol{a}} + \bar{\boldsymbol{n}}$$

Each line of $\bar{Z}$ is a line of the $M \times M$ identity matrix, so that

$$\forall i\ :\ \bar{z}_{ij} \in \{0,1\}\ ,\ \forall j\ ;\ \ \bar{z}_{i1} + \cdots + \bar{z}_{iM} = 1\ .$$

These restrictions are equivalent to

$$\forall i\ :\ \bar{z}_{ij}\left(1 - \bar{z}_{ij}\right) \leq 0,\ \bar{z}_{ij} \geq 0, \bar{z}_{ij} \leq 1\ ,\ \forall j\ ;\quad \bar{z}_{i1} + \cdots + \bar{z}_{iM} = 1\ . \tag{17}$$

Let us introduce $\overline{\boldsymbol{\mathcal{H}}} = \left(\bar{\mathcal{H}}_{ijk}\right)$ given by

$$\bar{\mathcal{H}}_{ijk} = \bar{H}_{ij}\bar{a}_k\ .$$

Then,

$$(\bar{\boldsymbol{H}}\bar{\boldsymbol{Z}}\bar{\boldsymbol{a}})_{\boldsymbol{i}} = \sum_{\boldsymbol{j,k}} \bar{H}_{ij}\bar{Z}_{jk}\bar{a}_k = \sum_{\boldsymbol{j,k}} \bar{\mathcal{H}}_{ijk}\bar{Z}_{jk}\ ,$$

and

$$\bar{\boldsymbol{H}}\bar{\boldsymbol{Z}}\bar{\boldsymbol{a}} = \overline{\boldsymbol{\mathcal{H}}}\overline{\boldsymbol{Z}}$$

14

Notice that $\overline{\boldsymbol{\mathcal{H}}}$ may be transformed into a matrix $\overline{\mathbb{H}}$ and $\overline{\boldsymbol{Z}}$ may be transformed into a vector $\overline{\mathbb{Z}}$ by using the correspondence $(j,k) \to \ell = j + 2(k-1)N_t$, $\overline{\mathbb{H}}_{i\ell} = \overline{\mathcal{H}}_{ijk}$, $\overline{\mathbb{Z}}_{\ell} = \bar{Z}_{jk}$. Then,

$$\overline{\boldsymbol{y}} = \overline{\boldsymbol{\mathcal{H}}}\overline{\boldsymbol{Z}} + \overline{\boldsymbol{n}} = \overline{\mathbb{H}}\overline{\mathbb{Z}} + \overline{\boldsymbol{n}} \tag{18}$$

Eq. (18) is analogous to Eq. (9), but restrictions (17) must be taken into account. Notice that Eqs. (17)-(18) may be solved for $(\overline{\boldsymbol{Z}}, \overline{\boldsymbol{n}})$. For instance, we may use a constrained least squares method may be used. We may also use algebraic equation methods: notice that Eq.(17) is equivalent to

$$\forall i \ : \ \bar{z}_{ij}\left(1 - \bar{z}_{ij}\right) = 0, \ \forall j \, ; \quad \bar{z}_{i1} + \cdots + \bar{z}_{iM} = 1 \, . \tag{19}$$

Thus, Eqs. (18)-(19) form a overdetermined nonlinear system which may be solved by adapted methods – eventually by a least squares approach. The number of unknowns is $2\,N_tM + 2N_r$, while the number of equations is $2\,N_t(M+1) + 2N_t$. A simplified approach may use the approximation

$$\overline{\boldsymbol{y}} \approx \boldsymbol{E}(\overline{\boldsymbol{y}}) = \overline{\boldsymbol{\mathcal{H}}}\overline{\boldsymbol{Z}} + \boldsymbol{E}(\overline{\boldsymbol{n}}) = \overline{\mathbb{H}}\overline{\boldsymbol{Z}} + \boldsymbol{E}(\overline{\boldsymbol{n}}) \tag{20}$$

Since $\boldsymbol{E}(\overline{\boldsymbol{n}})$ was previously estimated, Eq. (20) may be used in combination with Eq. (17) or Eq. (19) to furnish an estimation of $\overline{\boldsymbol{Z}}$ **.** The results may be corrected by replacing x_i by the closest member of $\boldsymbol{a}$:

$$x_i = a_{j(i)}, \ j(i) = \arg\min\{|x_i - a(j)| : 1 \le j \le M\} \tag{21}$$

A second approach, more simplified yet, consists in using the equation

$$\boldsymbol{H}^*\boldsymbol{E}(\boldsymbol{y}) = \boldsymbol{H}^*\boldsymbol{H}\boldsymbol{x} + \boldsymbol{H}^*\boldsymbol{E}(\boldsymbol{n}),$$

we have

$$\boldsymbol{x} = (\boldsymbol{H}^*\boldsymbol{H})^{-1}\boldsymbol{H}^*\big(\boldsymbol{E}(\boldsymbol{y}) - \boldsymbol{E}(\boldsymbol{n})\big) \approx (\boldsymbol{H}^*\boldsymbol{H})^{-1}\boldsymbol{H}^*\big(\boldsymbol{y} - \boldsymbol{E}(\boldsymbol{n})\big) \, . \tag{22}$$

The estimation furnished by Eq. (22) is corrected as indicated in Eq. (21).

Let us illustrate these approaches. Initially we consider $M = 2 \ (QAM4)$, $\boldsymbol{a} = \{-1,1\}$ and the message

$$\overline{\boldsymbol{x}} = \ (1,-1,1,-1,1,-1,1,-1,1,1,1,-1,-1,1,1,1,-1,-1)^t \, .$$

The noise is the same as in the preceding sections (uniformly distributed for the real part and Laplace distributed for the imaginary part). Initially, we determine the noise characteristics by the method exposed in section 3, using 1e4 measurements: this step furnishes also an estimation of $\boldsymbol{E}(\overline{\boldsymbol{n}})$. Then, we identify the channel matrix as indicated in section 4, using 1e3 measurements. We perform 1e4 estimations of the message using a different realization of the noise each time. The performance of the methods is shown in the **Figure 6**. The first approach produced the exact result in 100 % of the runs, while the second one produced the exact result in 90.4 % of the runs.

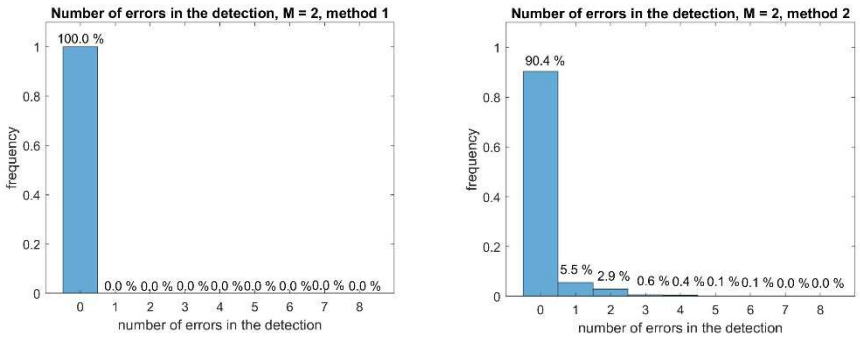

Fig. 6. Results for 1E4 runs. The alphabet has length 2 (QAM4). Method 1 has 100 % of success (no erroneous symbol). Method 2 finds all the exact symbols in 90.4 % of the runs.

Now, let us consider $M = 8\ (QAM64, d = 3)$, $\boldsymbol{a} = \{-7, -5, -3, -1, 1, 3, 5, 7\}$ and the message (randomly generated)

$$\overline{\boldsymbol{x}} = (-3, 3, 3, 7, 1, -7, 7, 1, -7, 1, 1, -3, 5, -7, 5, 7)^t .$$

Again, we realize 1e4 runs using distinct variates of the noise each time. The results are shown in the **Figure 7**. The first approach produced the exact result in 87 % of the runs, while the second one produced the exact result in 76 % of the runs.

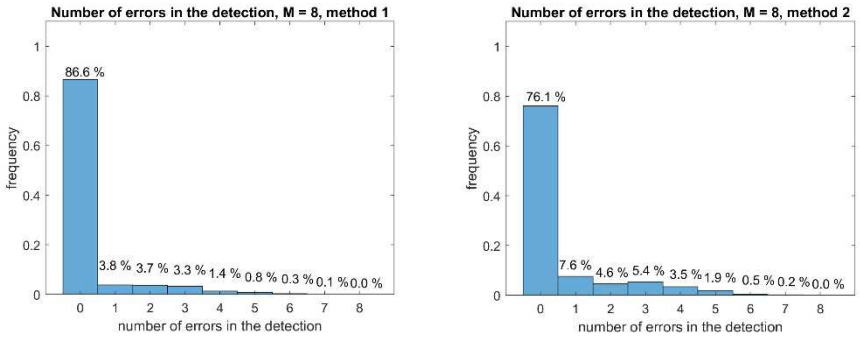

Fig. 7. Results for 1E4 runs, with an alphabet of length 8 (QAM64). Method 1 has no errors in 87 % of the runs. Method 2 in 76 %.

Then, let us consider $M = 32\ (d = 5)$, $\boldsymbol{a} = \{-31, -29, \ldots, -1, 1, \ldots, 29, 31\}$ and the message (randomly generated)

$$\overline{\boldsymbol{x}} = (7, 1, 15, 11, 15, -7, 21, 23, -19, -7, -9, 3, -23, -1, -29, 25)^t .$$

The performance of the methods is shown in the **Figure 8**. The first approach produced the exact result in 87 % of the runs, while the second one generally fails.

16

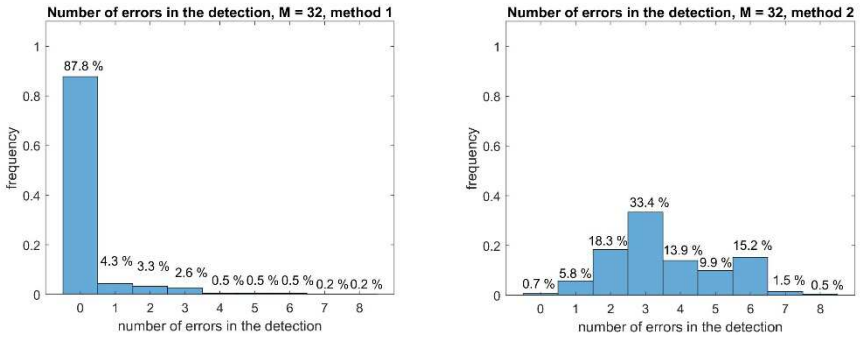

Fig. 8. Results for 1E4 runs and an alphabet of length 32. Method 1 has 88 % of success (no erroneous symbol). Method 2 generally fails.

Finally, let us consider $= \{-127, -125, \ldots, -1{,}1, \ldots, 125{,}129\}$, $M = 128$ $(d = 7)$, and the message (randomly generated)

$$\bar{\boldsymbol{x}} = (-117{,}65, -1, -27, -95{,}33, -43{,}59{,}13, -113{,}75{,}31{,}47, -95, -77{,}77)^t .$$

The performance of the method proposed is shown in the **Figure 9**: it produced the exact result in 87 % of the runs.

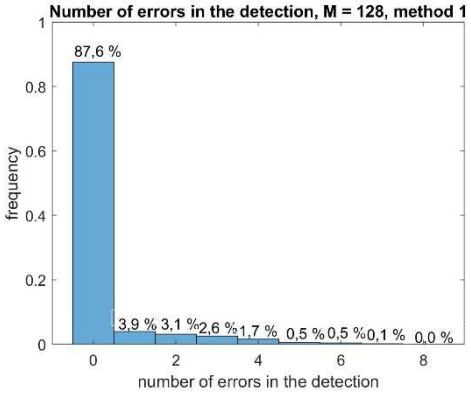

Fig. 9. Results for 1E4 runs. The alphabet has length 128 and spread is 2. Method 1 has 87.6 % of success (no erroneous symbol).

The performance of the methods depends on the spread of the alphabet, id est, of the distance between consecutive symbols: for instance, the alphabets considered up to this point have a spread of 2: the difference between consecutive symbols is 2 – what is the actual standard in telecommunications. As a prospective analysis, let us consider $= \{-15, -11, -7, -3{,}1{,}5{,}9, 13\}$, which corresponds to $M = 8$ with a spread of 4. Notice that the alphabet becomes asymmetric. We consider the message

$$\bar{\boldsymbol{x}} = (9{,}5{,}13{,}13, -7{,}1{,}5, -3{,}9, -11, -15, -15, -11{,}1{,}1, -3)^t .$$

This message corresponds to symbols in the same positions as in the test performed for the alphabet of length 8 in the preceding. The results are shown in **Figure 10** below: we observe that the performance of both the methods increase significantly: the method 1 has found all the correct symbols in 99.9 % of the runs.

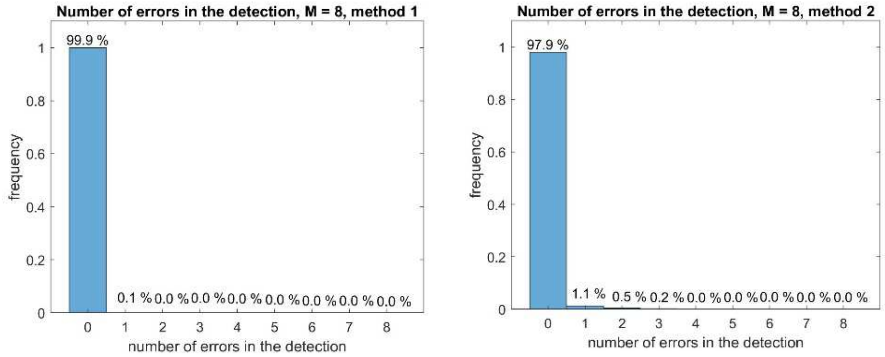

Fig. 10. Results for 1E4 runs of the method with an asymmetric alphabet spread out. The alphabet has length 8, and the spread is 4 (the double of the one initially considered). Method 1 has 99.9 % of success (no erroneous symbol) and method 1 has 97.9 % of success.

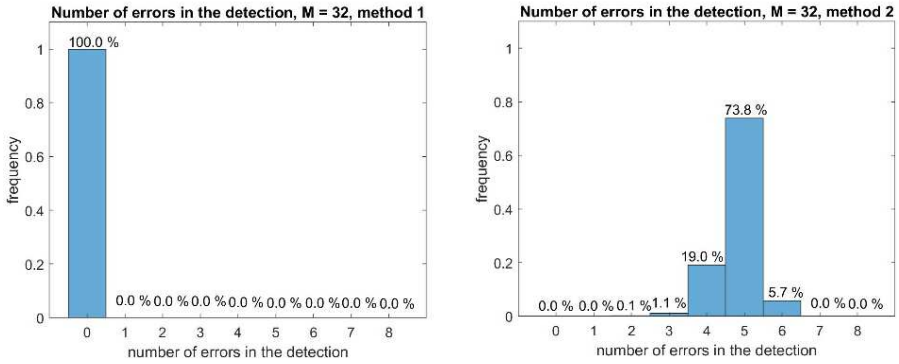

Fig. 11. Results for 1E4 runs of the method. The alphabet is asymmetric, of length 32, with a spread of 8. Method 1 has 100 % of success (no erroneous symbol). Method 2 generally fails.

A second example of the influence of the spread is given in **Figure 11** above. We consider $M = 32$ with an spread of 8: $\boldsymbol{a} = \{-127, -119, \dots, -7, 1, \dots, 113, 121\}$ and the message corresponding to symbols at the same positions as the used in the test previously presented for this alphabet:

$$\bar{\boldsymbol{x}} = (25, 1, 57, 41, 57, -71, -31, 81, 89, -79, -39, 9, -95, -7, -119, 97)^t .$$

The first approach produced the exact result in 100 % of the runs, while the second one fails.

It is also possible to consider symmetric alphabets with larger spread. For instance, $a = \{-14, -10, -6, -2, 2, 6, 10, 14\}$ is a symmetric alphabet of length 8, having a spread of 4. The effects of the spread are illustrated in the **Figure 12** below.

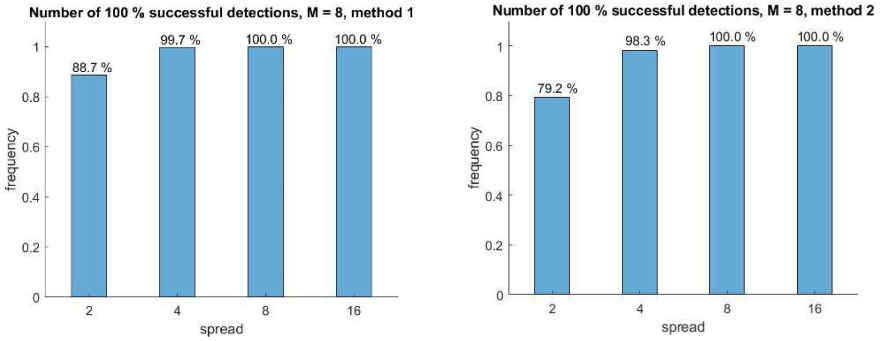

Fig. 12. Influence of the spread: results for 1E4 runs of the method. The alphabet is symmetric, of length 8. The rate of success increases for both the methods.

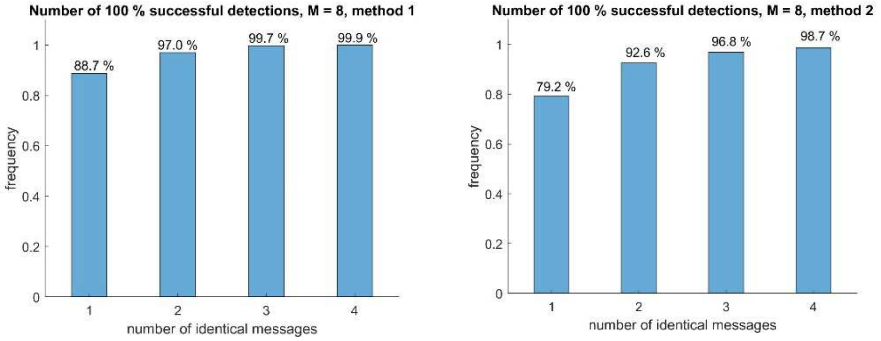

Fig. 13. Influence of the redundancy: results for 1E4 runs. The alphabet is symmetric, of length 8, spread 2. The rate of success increases with redundancy for both the methods.

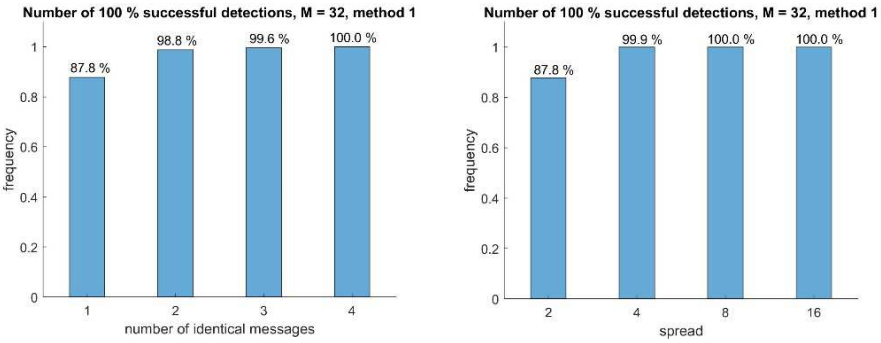

Fig. 14. Influence of the redundancy and spread: results for 1E4 runs. The alphabet is symmetric, of length 32. Redundancy analysis uses a fixed spread equal to 2. Spread analysis is made with no redundancy (a single sending). Method 2 fails in this case

The quality of the detection depends also upon the redundancy of the message. For instance, we may consider a simple redundancy implemented by sending r times the same message. The influence of r is illustrated in the **Figures 13** (above)**, 14** (above) **and 15** (below).

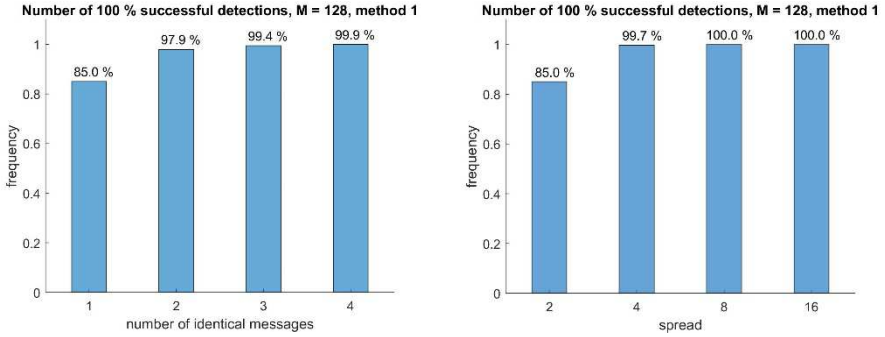

Fig. 15. Results for a symmetric alphabet of 128 symbols, 1E4 runs of the method. For the analysis of the effect of redundancy, the spread is fixed to 2. For the analysis of the effect of the spread, there is no redundancy (a single message without any repetition). For this alphabet, Method 2 fails.

6 Concluding Remarks

We presented an application of UQ approaches to a MIMO system. The resulting approach determines the distribution of the noise by using silent measurements. Then, it identifies the Channel Matrix by using pilots (id est, reference signals). Once these quantities were identified, the lecture of sequences of transmitted symbols is possible, by using identification techniques. In this work, we introduced a method of identification based on the determination of a selection matrix formed by lines of the identity matrix. We established statistics of the performance of the method by realizing the identification of the same sequence of symbols ten thousand times and drawing up the histograms of the number of errors in each identification. No correcting code was used in the tests, which show crude results, but we examined the effects of redundancy by considering repeated messages. We examine also the effects of the distance between symbols: the larger is the spread and the larger is the number of repetitions, the smaller are the errors: for convenient values, the rate of error is almost null – this is a prospective analysis, since the usual spread in telecommunications is 2. Two methods were considered: the faster one does not involve selection matrix but fails for alphabets using more than 8 symbols. The second method uses a selection matrix and appears as more robust. Several variations of the parameters were considered – for instance, changes in the number of measurements (divided by 10), using the rough estimation $\boldsymbol{E(n)} \approx \mathbf{0}$, using different methods of optimization, … - and led to analogous results. The preliminary results of this work may be considered as promising and encourage further research in the application of UQ approaches to MIMO systems.

References

1. Heath Jr, Robert W., and Angel Lozano. *Foundations of MIMO communication*. Cambridge University Press, 2018.
2. Huang, Yiteng, Jacob Benesty, and Jingdong Chen. "Identification of acoustic MIMO systems: Challenges and opportunities." *Signal Processing* 86.6 (2006): 1278-1295.
3. Li, Baosheng, et al. "MIMO-OFDM for high-rate underwater acoustic communications." *IEEE Journal of Oceanic Engineering* 34.4 (2009)
4. Zhang, Ling, Ming Li, and Gangsheng Li. "Symbol estimation for MIMO underwater acoustic communication based on multiplicative noise model." *2014 IEEE International Conference on Communiction Problem-solving*. IEEE, 2014.
5. Zhang, Ling, et al. "Symbol estimation algorithm for MIMO underwater acoustic communication system based on multiplicative noise model." *Mathematical Problems in Engineering* 2015 (2015).
6. Barhumi, Imad, Geert Leus, and Marc Moonen. "Optimal training design for MIMO OFDM systems in mobile wireless channels." *IEEE Transactions on signal processing* 51.6 (2003): 1615-1624.
7. Lopez, R. H; . Souza de Cursi, J. E.; Lemosse, D.: Approximating the probability density function of the optimal point of an optimization problem, Engineering Optimization, 43:3, 281-303, DOI: 10.1080/0305215X.2010.489607 (2011)
8. Lopez, R. H.; Miguel, L. ; Souza de Cursi, E.: Uncertainty quantification for algebraic systems of equations. Computers and Structures. 128. 189-202. 10.1016/j.compstruc.2013.06.016 (2013).
9. Lopez, R. H.; Souza de Cursi, E.; Carlon, A.: A state estimation approach based on stochastic expansions. Computational and Applied Mathematics. 10.1007/s40314-017-0515-0 (2017).
10. Souza de Cursi, E.; Sampaio, R. : Uncertainty Quantification and Stochastic Modeling with Matlab. Elsevier Science Publishers B. V., NLD (2015)
11. Souza de Cursi, E. : Variational methods for engineers with Matlab. ISTE, Ltd. ; Hoboken, NJ ; Wiley, London, UK. (2015)